

Phase dynamics of inhomogeneous Manakov vector solitons

N. M. Musammil,^{1,*} P. A. Subha,^{2,†} and K. Nithyanandan^{3,‡}

¹*Department of Physics, Calicut University, Malappuram, Kerala-673635, India*

²*Department of Physics, Farook College, Calicut University, Kerala-673632, India*

³*Laboratoire Interdisciplinaire de Physique, UMR 5588 CNRS, Université Grenoble Alpes, Saint Martin de Heres, France*



(Received 26 October 2018; revised manuscript received 27 March 2019; published 25 July 2019)

We report the exact phase dynamics of Manakov bright and dark vector solitons in an inhomogeneous optical system by means of a variable coefficient coupled nonlinear Schrödinger equation. To investigate the phase dynamics, we have modified the Manakov system with a relation between two modes of propagation, that are obtained by the Hirota bilinear method. The importance of the phase study in soliton interaction is revealed by asymptotic analysis of two-soliton solutions. In contrast with the Manakov bright soliton, the time-dependent dark vector soliton exhibits a gradual phase shift due to the blackness factor. The various inhomogeneous effects on the soliton phase are investigated, with a particular emphasis on nonlinear tunneling. The intensity and corresponding phase of the tunneling soliton either forms a peak or valley and retains its shape after tunneling. Unlike the bright counterpart, the gain or loss term significantly affects the phase of the dark soliton. Apart from the study of soliton intensity, the phase profile of bright and dark vector solitons and its dynamical features are also explored. As the study is not limited to intensity description, the present study could serve as a reference for the future studies on multisolitons phase dynamics in photonics and related fields.

DOI: [10.1103/PhysRevE.100.012213](https://doi.org/10.1103/PhysRevE.100.012213)

I. INTRODUCTION

One of the most elegant and simplest form of integrable coupled nonlinear Schrödinger (CNLS) equation describing the copropagation of intense optical beams in the two-components birefringent system is the so-called Manakov model [1]. The effect of birefringence in a single-mode fiber was first considered by Menyuk [2]. The formation and different dynamical features of optical solitons, including the possibility of soliton-driven large-scale communication network, are widely discussed in Refs. [1–10]. The ideal soliton propagation without any attenuation in monomode optical fiber is governed by the nonlinear Schrödinger (NLS) equation. Nevertheless, in many real situations, there exist two different polarizations in single-mode fibers, which split the injected soliton into two separate beams. The coupling of this bimodal propagation of pulse results in many fascinating phenomena, one of which is the vector soliton. Usually, the walk-off effect due to the group-velocity mismatch between the bimodal solitons cannot be neglected from the description of two or more closely spaced optical pulses. However, the copropagation of two orthogonally polarized solitons can be realized by the soliton trapping mechanism [11–13]. This unsplit two-component soliton by the soliton trapping technique is generally referred to as a vector soliton. The coupled NLS equation provides a quantitative description of such copropagating solitons via the cross-phase modulation mechanism [14,15].

The existence of two-component vector soliton in birefringent Kerr medium was first proposed by Manakov [16]. The utility of these theoretical model can be employed under a specific choice of nonlinear parameters, that is, the cross-coupling coefficient must be equal to unity and the self-phase modulation coefficients need to be equal for both polarizations. It is a well-known integrable model of CNLS equation, which yields an explicit form of the stable multisoliton solution in different fields. The experimental possibility of the Manakov model with a specially fabricated birefringent optical fiber has been discussed by Menyuk [14]. Following the seminal work, several interesting experiments for the physical realization of Manakov-like solitons were reported, including photorefractive crystals [12,13,17–19], semiconductor waveguide [20], quadratic media [21], optical fiber [14], and Bose-Einstein condensates [22]. Also, polarization modulation instability in a Manakov fiber system was studied by Frisquet *et al.* in Ref. [23]. Recently, the Manakov vector soliton has attracted renewed interest among the researchers due to its important applications in optical fiber systems such as optical switching and soliton dragging logic gates [24–28]. By deriving an explicit two-soliton solution for the Manakov system, Radhakrishnan *et al.* [24] observed the intensity redistribution (energy-exchange) between the two component fields. Experimentally, energy-exchanging collisions [17] and information transfer [18] were also realized in photorefractive crystals. Moreover, there exist several interesting theoretical studies on Manakov solitons, including quantum theory of Manakov solitons [29], multisoliton perturbation theory for the Manakov equations [30], soliton trapping, and daughter waves in the Manakov model [15].

Based on the different signs of group velocity dispersion (GVD) parameter, the Manakov model mainly admits two

* musammilnm7007@gmail.com

† Corresponding author: pasubha@gmail.com

‡ nithi.physics@gmail.com

kinds of vector soliton propagation, bright and dark, respectively. The bright (dark) vector soliton in the anomalous (normal) dispersion regime was thoroughly investigated in many pioneering works [31,32]. The key features of the Manakov bright-bright pair is the energy sharing collision between the components of the interacting vector solitons. But in the case of a dark-dark pair, it always exhibits an elastic mode of interactions [33,34]. In most of the previous studies reported in the context of the Manakov model, the interaction dynamics and the discussion was primarily based on the intensity description, only a little emphasize is paved on the phase dynamics. In the present context, in addition to the intensity based explanations, we highlight and discuss the phase dynamics of the Manakov soliton for the first time to the best of our knowledge. For a complete understanding of the system dynamics, it would be interesting to reveal the distinct properties of intensity and their corresponding phase profile of Manakov bright and dark solitons. We further extend the phase analysis to the case of multisoliton interactions and highlight the variation of phase for different soliton types.

Most of the investigation on the Manakov model was based on the coupled NLS under a consideration that the optical fiber maintains the fiber parameters during the propagation of light. However, in the realistic optical fiber under practical conditions, the medium exhibits an inevitable inhomogeneous behavior. The variable coefficient CNLS equations (Vc-CNLSE) serves as the practical model to describe the vector soliton dynamics in inhomogeneous systems [35–37]. In this work, we focus on the following Vc-CNLSE model of a two-coupled system with distributed dispersion, nonlinearity, and gain or loss which can also be referred as inhomogeneous Manakov model [34,38–40]:

$$iq_{1z} \pm \frac{1}{2}V(z)q_{1tt} + R(z)(|q_1|^2 + |q_2|^2)q_1 + ip(z)q_1 = 0, \quad (1a)$$

$$iq_{2z} \pm \frac{1}{2}V(z)q_{2tt} + R(z)(|q_2|^2 + |q_1|^2)q_2 + ip(z)q_2 = 0, \quad (1b)$$

where $q_1(z, t)$ and $q_2(z, t)$ are the complex envelopes for the two polarization components in Kerr medium. The variables z and t represent the normalized spatial and temporal coordinates. The group velocity dispersion, Kerr nonlinearity, and gain or absorption effects are related to the respective coefficient functions $V(z)$, $R(z)$, and $p(z)$. By using Hirota's bilinear (HB) method, we analytically derived the exact solutions for the Eq. (1), which also provides an explicit form of multisoliton solutions. In this work, apart from the intensity, we reveal the influence of inhomogeneity on the phase of the Manakov solitons for the first time to the best of our knowledge. The given model Eq. (1) has the capability to handle many inhomogeneous behaviors in fiber such as pulse gain or absorption, background oscillation, pulse compression, dispersion-managed transmission systems, and nonlinear tunneling. The vector soliton phase has not been studied analytically so far, and, being motivated by this fact, we paid particular attention to soliton propagation and corresponding phase change with constant or varying coefficients. Unlike the bright counterpart, the phase of dark vector soliton gives

more intriguing results and the interaction scenario provides interesting features which have not been reported so far.

The organization of the paper is as follows. In Sec. II, we derive an exact bright and dark Manakov vector soliton solutions by HB method. Section III describe the phase dynamics of Manakov one-soliton solutions. A two-soliton solution and soliton collision by employing asymptotic analysis are presented in Sec. IV. A brief discussion about the various physical effects in intensity and corresponding phase dynamics of vector soliton propagation through an inhomogeneous medium is reported in Sec. V. The paper concludes with a summary of results in Sec. VI.

II. EXACT SOLITON SOLUTIONS BY HB METHOD

To obtain exact vector soliton solutions of Eq. (1), we use the HB method [41–44], which is expected to give an explicit form of bright and dark multisoliton solutions, as follows:

$$q_1(z, t) = g(z)\frac{G}{F}, \quad (2a)$$

$$q_2(z, t) = g(z)\frac{H}{F}, \quad (2b)$$

where G and H are complex functions and F is a real function. By substituting this transformation into Eq. (1), the following bilinear equations can be obtained,

$$[iD_z \pm \frac{1}{2}V(z)D_t^2 + \lambda(z)](G \cdot F) = 0, \quad (3a)$$

$$[iD_z \pm \frac{1}{2}V(z)D_t^2 + \lambda(z)](H \cdot F) = 0, \quad (3b)$$

$$\delta(|G|^2 + |H|^2) \mp D_t^2(F \cdot F) = \frac{2\lambda(z)}{V(z)}F^2, \quad (3c)$$

where $\delta(z) = \frac{2R(z)}{V(z)}g(z)^2$ and D_z and D_t are the bilinear differential operators [41] defined by

$$D_z^m D_t^n (g \cdot f) = \left(\frac{\partial}{\partial z} - \frac{\partial}{\partial z'} \right)^m \left(\frac{\partial}{\partial t} - \frac{\partial}{\partial t'} \right)^n \times g(z, t)f(z', t')|_{z'=z, t'=t}.$$

With the condition $g_z(z) + g(z)p(z) = 0$, we can choose $\lambda(z) = 0$ for the bright soliton solution. But, for the dark soliton case, $\lambda(z)$ is an analytic function to be determined.

A. Bright one-soliton solutions

The bright multisoliton solutions of Eq. (1) can be generated by solving the above set of Eqs. (3) with the power-series expansions of G and F as

$$G = \varepsilon^1 g_1 + \varepsilon^3 g_3 + \varepsilon^5 g_5 + \dots$$

$$H = \varepsilon^1 h_1 + \varepsilon^3 h_3 + \varepsilon^5 h_5 + \dots$$

$$F = 1 + \varepsilon^2 f_2 + \varepsilon^4 f_4 + \varepsilon^6 f_6 + \dots$$

with ε as the formal expansion parameter. In order to get the bright one-soliton solution, the power-series expansions for G , H , and F are truncated corresponding to the lowest order in ε as follows: $G = g_1$, $H = h_1$, and $F = 1 + f_2$. Then, back to

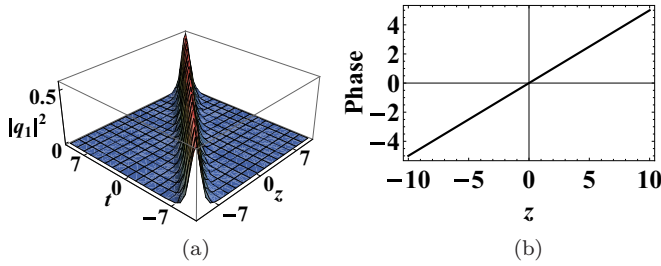


FIG. 1. The bright soliton propagation through a constant fiber medium for parameters (a) $k_1 = 1 + i$, $\alpha_1 = 1 + i$, $\beta_1 = 2 - i$, $V(z) = 1$, $R(z) = 0.5$, and $p = 0$. (b) Corresponding phase profile.

bilinear Eqs. (3), we obtain

$$\begin{aligned}
 g(z) &= e^{-\int p(z)dz} & g_1 &= \alpha_1 e^{\theta_1} \\
 h_1 &= \beta_1 e^{\theta_1} & f_2 &= \varrho_1 e^{\theta_1 + \theta_1^*} \\
 \theta_1 &= k_1 t - \omega_1 \int V(z)dz + \phi_1 & \omega_1 &= -\frac{1}{2} i k_1^2 \\
 \varrho_1 &= \frac{\delta(|\alpha_1|^2 + |\beta_1|^2)}{2(k_1 + k_1^*)^2}.
 \end{aligned}$$

Thus, bright one-soliton solutions can be written as

$$\begin{pmatrix} q_1 \\ q_2 \end{pmatrix} = \begin{pmatrix} \alpha_1 \\ \beta_1 \end{pmatrix} \frac{e^{-\int p(z)dz}}{2\sqrt{\varrho_1}} e^{-i\theta_1 t} \operatorname{sech}\left(\theta_1 t + \frac{\ln \varrho_1}{2}\right). \quad (4)$$

From Eq. (4), we can analyze the characteristics of bright one-soliton pulse in the inhomogeneous fibers. Here α_1 and β_1 are the arbitrary complex parameters which determine the amplitude of the bright soliton. k_{1R} and k_{1I} represent the real and imaginary parts of the complex parameter k_1 , which determine the amplitude and velocity of solitons. The bright soliton propagation through constant fiber is depicted in Fig. 1(a).

B. Dark one-soliton solutions

We obtain the dark one-soliton solution by truncated series of G , H , and F to the lowest order in ε as follows: $G = g_0(1 + \varepsilon g_1)$, $H = h_0(1 + \varepsilon h_1)$, and $F = 1 + \varepsilon f_1$. Here we assume

$$\begin{aligned}
 g_0 &= a e^{i\phi} & h_0 &= b e^{i\phi} \\
 g_1 &= \mu_1 e^{\theta_1} & h_1 &= \nu_1 e^{\theta_1} \\
 f_1 &= e^{\theta_1} & g(z) &= e^{-\int p(z)dz} \\
 \phi &= k_0 t - \omega_0 \int V(z)dz & \theta_1 &= k_1 t - \omega_1 \int V(z)dz + \phi_1.
 \end{aligned}$$

Then, back to bilinear Eqs. (3), we obtain some associated parameters related to one-soliton solutions as

$$\begin{aligned}
 \lambda &= \frac{1}{2} \delta(a^2 + b^2)V(z) & \omega_0 &= -\frac{\lambda}{V(z)} - \frac{k_0^2}{2} \\
 \mu_1 &= \frac{2\omega_1 + 2k_0 k_1 + i k_1^2}{2\omega_1 + 2k_0 k_1 - i k_1^2} & \mu_1 &= \nu_1 \\
 \omega_1 &= \frac{k_1}{2} [-2k_0 \pm \sqrt{2\delta(a^2 + b^2) - k_1^2}].
 \end{aligned}$$

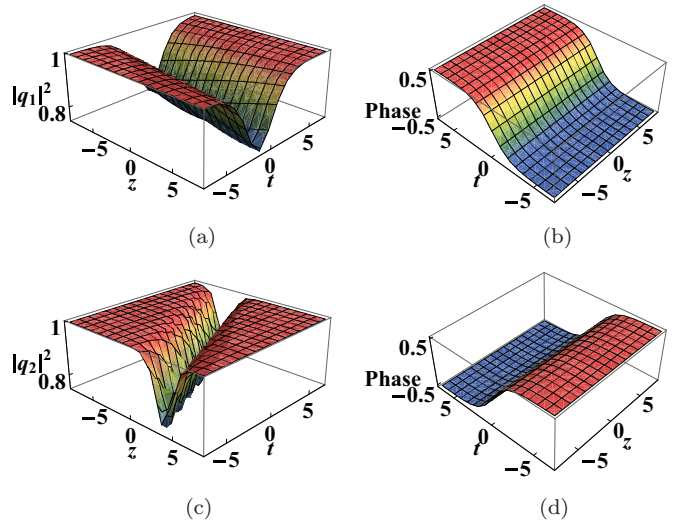


FIG. 2. The dark soliton propagation through homogenous fiber for parameters. (a) $k_1 = 1$. (b) Corresponding phase profile. (c) $k_1 = -1$. (d) Corresponding phase profile. Other physical quantities are $a = b = 1 = k_0 = V(z) = \delta = 1$.

The dark one-soliton solutions can be written as

$$\begin{pmatrix} q_1 \\ q_2 \end{pmatrix} = \begin{pmatrix} a \\ b \end{pmatrix} \frac{(1 + \mu_1) + (\mu_1 - 1) \tanh\left(\frac{\theta_1}{2}\right)}{2e^{\int p(z)dz} e^{-i\phi}}. \quad (5)$$

From Eq. (5), one can analyze the dynamics of vector dark one-soliton pulse in the inhomogeneous fibers. The propagation of dark one-soliton through the inhomogeneous fiber is depicted in the Fig. 2.

1. Parametric region for black and gray soliton

The amplitude (A_j), blackness parameter (B_j), and background wave amplitude (a or b) are connected by a simple relation $A_j^2 + B_j^2 = a^2(b^2)e^{-2\int p(z)dz}$ [7]. Based on the parameter A_j or B_j of the obtained solutions, the dark soliton can be classified into black and gray mode of soliton. In principle, the dark soliton with zero intensity at its center is referred to as the black soliton [$B_j^2 = a^2(b^2)e^{-2\int p(z)dz}$], all other dark soliton cases with nonzero intensity at the pulse center are all identified as [$B_j^2 < a^2(b^2)e^{-2\int p(z)dz}$] as gray solitons [45–47]. In Fig. 3, we have plotted the black and gray soliton with different blackness parameter.

To explore the dynamics of dark soliton propagation given by Eq. (5), some of the physical quantities such as velocity [$v = \frac{\omega_1}{k_1} V(z)$], amplitude ($A_1^1 = \left(\frac{a}{b}\right) \left|\frac{(1+\mu_1)}{2e^{\int p(z)dz}}\right|$), and blackness factor ($B_2^1 = \left(\frac{b}{a}\right) \left|\frac{(\mu_1-1)}{2e^{\int p(z)dz}}\right|$) are important. The dark vector soliton energy associated with blackness factor can be written as [47]

$$E_1 = \int_{-\infty}^{\infty} (a^2 - |q_1|^2) dt = \frac{4B_1^2}{k_1 e^{2\int p(z)dz}}, \quad (6a)$$

$$E_2 = \int_{-\infty}^{\infty} (b^2 - |q_2|^2) dt = \frac{4B_2^2}{k_1 e^{2\int p(z)dz}}. \quad (6b)$$

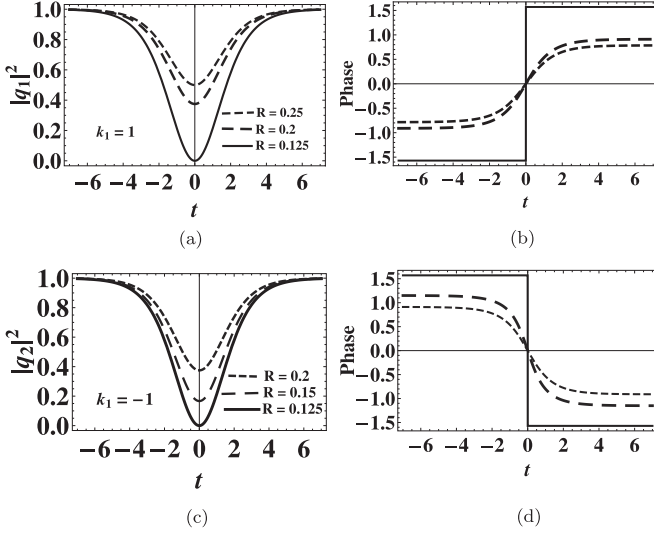


FIG. 3. The black and gray soliton with different values of blackness factor. (a) $k_1 = 1$ and $R = 0.125, 0.2, 0.25$. (b) Corresponding phase profile. (c) $k_1 = -1$ and $R = 0.125, 0.15, 0.2$. (d) Corresponding phase profile. Other physical quantities are $a = b = 1 = k_0 = V(z) = 1$.

C. Direct numerical simulation

The stability of soliton solutions is of paramount importance for its application and physical feasibility. Unlike the conventional pulses of different form, the solitons are relatively stable, even in an environment subjected to external perturbations. Hence, in order to validate the signature of soliton, such as stable propagation over appreciable distance, and the stability against perturbation, we perform numerical simulation using split-step Fourier method. In order to check the solution stability of our dark soliton solutions, as a representative case, we consider the one soliton solution corresponding to both bright and dark soliton given respectively by Eqs. (4) and (5). The stability analysis is performed in two parts, (i) direct numerical simulation of propagation of soliton using Vc-CNLSE and (ii) the propagation of soliton

subjected to perturbation such as the photon noise. Figures 4 and 5 show the numerical simulation of stable propagation of the bright and dark soliton propagation. Figure labeled “a” on top corresponds to the propagation without noise, while the figure labeled “b” is the propagation under noise perturbation. Figures 4(b) and 5(b) represent the contour plot of Figs. 4(a) and 5(a), respectively.

In principle, the propagation of soliton pulse in a fiberlike media is typically subjected to environmental fluctuations, and there are numerous effects that can contribute to instability. Therefore, it is very informative to study the stability of the soliton in an environment subject to external noise or perturbations. We numerically generated a photon white noise, which corresponds to 0.035% of the soliton or background intensity. This is indeed an appreciable noise level, which can potentially perturb any propagation. The initial condition for the simulation is the soliton profile given by Eqs. (4) and (5) along with synthesized numerical noise. It is very evident from the figures labeled “b” that both bright and dark solitons show remarkable stability against strong perturbation. Thus, one can draw out a conclusion that the soliton solution constructed through the Hirota method shows excellent stability, which has been confirmed through direct numerical simulations.

III. PHASE DYNAMICS OF MANAKOV SOLITON

From the exact solutions given by Eqs. (4) and (5) for bright and dark solitons, respectively, we arrive at a relation between two modes of propagation as $q_1 = \frac{M}{N}q_2$, where M and N replace $\alpha_1(a)$ and $\beta_1(b)$ and the modified Eq. (1) can be given as

$$iq_{1z} \pm \frac{1}{2}V(z)q_{1tt} + R(z)\left(1 + \frac{|N|^2}{|M|^2}\right)q_1|q_1|^2 + ip(z)q_1 = 0, \quad (7a)$$

$$iq_{2z} \pm \frac{1}{2}V(z)q_{2tt} + R(z)\left(1 + \frac{|M|^2}{|N|^2}\right)q_2|q_2|^2 + ip(z)q_2 = 0. \quad (7b)$$

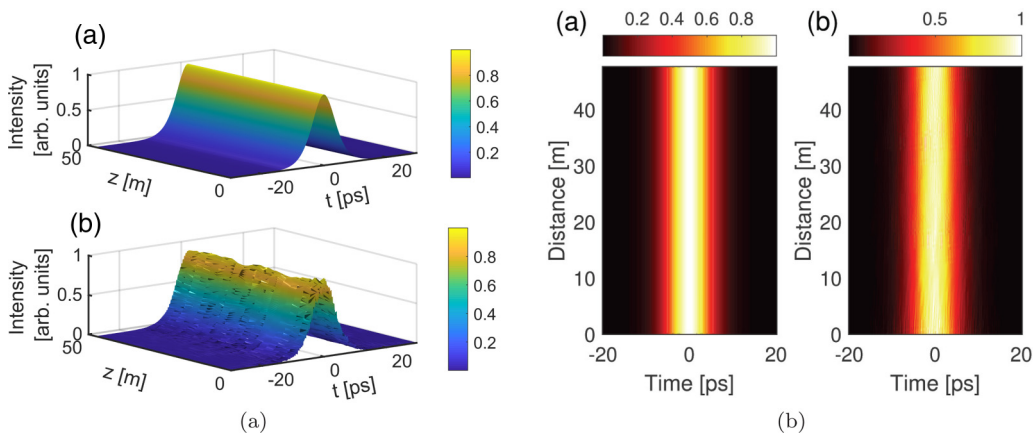


FIG. 4. The propagation of bright soliton along the fiber. The left panel represents the evolution of the bright soliton pulse and the influence of noise, while the panel right portrays the contour evolution.

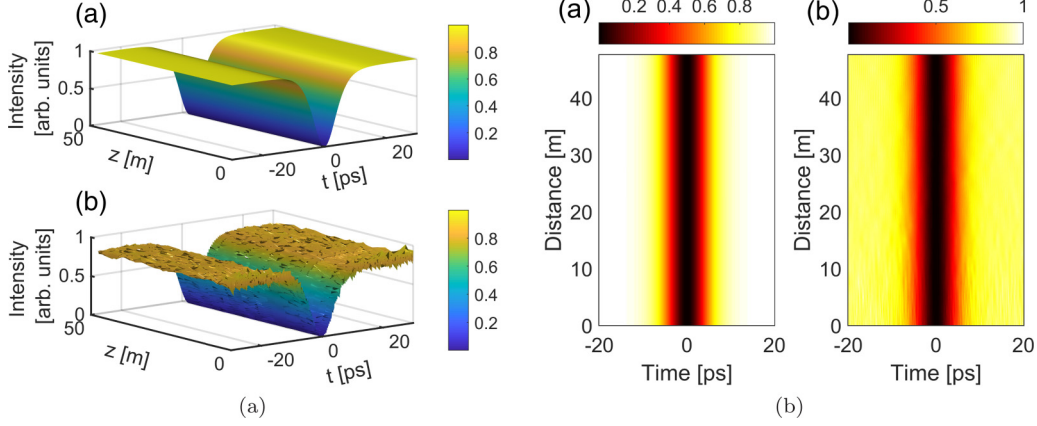


FIG. 5. The propagation of dark soliton along the fiber. The left panel represents the evolution of the dark soliton pulse and the influence of noise, while the panel right portrays the contour evolution.

To obtain the phase of Manakov soliton, first we introduce the solution as given below

$$q_1(z, t) = \rho_1(z, t)e^{i\psi_1(z, t)}, \quad (8a)$$

$$q_2(z, t) = \rho_2(z, t)e^{i\psi_2(z, t)}. \quad (8b)$$

Substituting this expression into Eq. (7) and separating the real and imaginary parts, we obtain

$$\rho_{1z} + p(z)\rho_1 \pm V(z)\rho_{1t}\psi_{1t} + \frac{V(z)}{2}\psi_{1tt} = 0, \quad (9a)$$

$$\rho_{2z} + p(z)\rho_2 \pm V(z)\rho_{2t}\psi_{2t} + \frac{V(z)}{2}\psi_{2tt} = 0, \quad (9b)$$

$$2R(z)\left(1 + \frac{|N|^2}{|M|^2}\right)\rho_1^3 \pm V(z)\rho_{1tt} \mp V(z)\rho_1\psi_{1t}^2 - 2\rho_1\psi_{1z} = 0, \quad (10a)$$

$$2R(z)\left(1 + \frac{|M|^2}{|N|^2}\right)\rho_2^3 \pm V(z)\rho_{2tt} \mp V(z)\rho_2\psi_{2t}^2 - 2\rho_2\psi_{2z} = 0. \quad (10b)$$

The stationary condition for $|q_j|^2$ gives us an expression $\rho_{jz} + p(z)\rho_j = 0$, from which one can deduce $\rho_j = \rho_{0j} e^{-\int p(z)dz}$, where ρ_{0j} represent the amplitude of pulse without gain or loss. Further, by using Eq. (9), we obtain a phase relation $\psi_j = \int \frac{c_j(z)}{\rho_{0j}} dt + A_j(z)$, where $c_j(z)$ and $A_j(z)$ are integration constants. Assuming $\frac{dA_j}{dz}$ as a constant Ω_j , the expression for phase can be written as

$$\psi_j = \int \frac{c_j(z)}{\rho_{0j}^2} dt + \Omega_j z, \quad j = 1, 2. \quad (11)$$

Substituting the expression of phase (11) into (10), we obtain the following equation for $I_{0j} = |\rho_{0j}|^2$:

$$\left(\frac{dI_{01}}{dt}\right)^2 = \mp 2\delta\left(1 + \frac{|N|^2}{|M|^2}\right)I_{01}^3 \pm \frac{8\Omega_1}{V(z)}I_{01}^2 + 4K_1I_{01} - 4c_1^2, \quad (12a)$$

$$\left(\frac{dI_{02}}{dt}\right)^2 = \mp 2\delta\left(1 + \frac{|M|^2}{|N|^2}\right)I_{02}^3 \pm \frac{8\Omega_2}{V(z)}I_{02}^2 + 4K_2I_{02} - 4c_2^2, \quad (12b)$$

where $\delta(z) = \frac{2R(z)}{V(z)}e^{-2\int p(z)dz}$ and K_i is an integration constant. For bright soliton both c_j and K_j can be considered as zero. Hence the above expression can be cast into the form

$$\left(\frac{dI_{01}}{dt}\right)^2 = -2\delta\left(1 + \frac{|\beta_1|^2}{|\alpha_1|^2}\right)I_{01}^2(I_{01} - \rho_{1s}), \quad (13a)$$

$$\left(\frac{dI_{02}}{dt}\right)^2 = -2\delta\left(1 + \frac{|\alpha_1|^2}{|\beta_1|^2}\right)I_{02}^2(I_{02} - \rho_{2s}), \quad (13b)$$

where

$$\rho_{1s} = \frac{4\Omega_1}{\delta V(z)\left(1 + \frac{|\beta_1|^2}{|\alpha_1|^2}\right)}, \quad \rho_{2s} = \frac{4\Omega_2}{\delta V(z)\left(1 + \frac{|\alpha_1|^2}{|\beta_1|^2}\right)}. \quad (14)$$

By integrating Eq. (13), we obtain the intensity $I_j = I_{0j}e^{-2\int p(z)dz}$ as

$$I_1 = \rho_{1s}e^{-2\int p(z)dz} \text{Sech}^2\left[\sqrt{\frac{\delta}{2}\rho_{1s}\left(1 + \frac{|\beta_1|^2}{|\alpha_1|^2}\right)}t\right], \quad (15a)$$

$$I_2 = \rho_{2s}e^{-2\int p(z)dz} \text{Sech}^2\left[\sqrt{\frac{\delta}{2}\rho_{2s}\left(1 + \frac{|\alpha_1|^2}{|\beta_1|^2}\right)}t\right], \quad (15b)$$

comparing by these bright soliton intensities with the exact solutions given by Eq. (4), we have $(\rho_{2s}) = \frac{|\alpha_1|^2}{|\beta_1|^2} \frac{1}{4\varrho_1}$. Thus, the phase for bright vector soliton can be written as

$$\psi_j = \frac{\delta(|\alpha_1|^2 + |\beta_1|^2)V(z)}{16\varrho_1}z. \quad (16)$$

This shows that the phase of bright vector soliton depends only on the spatial coordinate, and the phase remains constant across the entire pulse. But in the variable coefficient model, the GVD parameter $V(z)$ significantly influences the soliton phase.

For the dark vector soliton the Eq. (12) can be cast into the form

$$\left(\frac{dI_{01}}{dt}\right)^2 = 2\delta\left(1 + \frac{|b|^2}{|a|^2}\right)(I_{01} - \rho_{1a})^2(I_{01} - \rho_{1b}), \quad (17a)$$

$$\left(\frac{dI_{02}}{dt}\right)^2 = 2\delta\left(1 + \frac{|a|^2}{|b|^2}\right)(I_{01} - \rho_{2a})^2(I_{02} - \rho_{2b}). \quad (17b)$$

Here ρ_{ja} and ρ_{jb} correspond to the double root and the single root of Eq. (12), respectively. By integrating Eq. (12), the intensity profile of dark one-soliton solution for Vc-CNLSE can be written as

$$|q_1|^2 = I_1 = \rho_{1a}e^{-2\int p(z)dz} \left\{ 1 - m_1^2 \operatorname{sech}^2 \left[\sqrt{\frac{\delta}{2}} \left(1 + \frac{|b|^2}{|a|^2} \right) \rho_{1a} m_1 t \right] \right\}, \quad (18a)$$

$$|q_2|^2 = I_2 = \rho_{2a}e^{-2\int p(z)dz} \left\{ 1 - m_2^2 \operatorname{sech}^2 \left[\sqrt{\frac{\delta}{2}} \left(1 + \frac{|a|^2}{|b|^2} \right) \rho_{2a} m_2 t \right] \right\}, \quad (18b)$$

where $m_j^2 = \frac{\rho_{ja} - \rho_{jb}}{\rho_{ja}}$. By equating Eq. (17) and (12), we get the following set of relations:

$$\Omega_1 = \frac{\delta}{4} \left(1 + \frac{|b|^2}{|a|^2} \right) \rho_{1a} (3 - m_1^2) V(z), \quad (19)$$

$$\Omega_2 = \frac{\delta}{4} \left(1 + \frac{|a|^2}{|b|^2} \right) \rho_{2a} (3 - m_2^2) V(z), \quad (20)$$

$$c_1^2 = \frac{\delta}{4} \left(1 + \frac{|b|^2}{|a|^2} \right) \rho_{1a}^3 (1 - m_1^2), \quad (21)$$

$$c_2^2 = \frac{\delta}{4} \left(1 + \frac{|a|^2}{|b|^2} \right) \rho_{2a}^3 (1 - m_2^2), \quad (22)$$

$$K_1 = \frac{\delta}{4} \left(1 + \frac{|b|^2}{|a|^2} \right) (\rho_{1a}^2 + 2\rho_{1a}\rho_{1b}), \quad (23)$$

$$K_2 = \frac{\delta}{4} \left(1 + \frac{|a|^2}{|b|^2} \right) (\rho_{2a}^2 + 2\rho_{2a}\rho_{2b}), \quad (24)$$

with these expressions, the phase of a dark soliton via Eq. (11) can be written as

$$\begin{aligned} \psi_1 = & \sqrt{\frac{\delta}{2} \left(1 + \frac{|b|^2}{|a|^2} \right) (1 - m_1^2) \rho_{1a} t} \\ & + \tan^{-1} \left\{ \frac{m_1 \tanh \left[\sqrt{\frac{\delta}{2}} \left(1 + \frac{|b|^2}{|a|^2} \right) \rho_{1a} m_1 t \right]}{\sqrt{1 - m_1^2}} \right\} + \Omega_1 z, \end{aligned} \quad (25)$$

$$\begin{aligned} \psi_2 = & \sqrt{\frac{\delta}{2} \left(1 + \frac{|a|^2}{|b|^2} \right) (1 - m_2^2) \rho_{2a} t} \\ & + \tan^{-1} \left\{ \frac{m_2 \tanh \left[\sqrt{\frac{\delta}{2}} \left(1 + \frac{|a|^2}{|b|^2} \right) \rho_{2a} m_2 t \right]}{\sqrt{1 - m_2^2}} \right\} + \Omega_2 z. \end{aligned} \quad (26)$$

It is interesting to note that Eq. (18) is almost same with the dark vector one-soliton solution [Eq. (5)] derived by HB

method. The intensity of dark soliton via Eq. (5) can be written as

$$|q_1|^2 = a^2 e^{-2\int p(z)dz} \left[1 - \frac{B_1^2}{a^2} e^{2\int p(z)dz} \operatorname{sech}^2 \left(\frac{k_1}{2} \right) \right], \quad (27a)$$

$$|q_2|^2 = b^2 e^{-2\int p(z)dz} \left[1 - \frac{B_2^2}{b^2} e^{2\int p(z)dz} \operatorname{sech}^2 \left(\frac{k_1}{2} \right) \right]. \quad (27b)$$

Here, by equating the parameters $a^2 = \rho_{1a}$, $b^2 = \rho_{2a}$, $\frac{B_1^2}{a^2} e^{2\int p(z)dz} = m_1^2$, and $\frac{B_2^2}{b^2} e^{2\int p(z)dz} = m_2^2$, we observed that the given expressions for intensity [Eqs. (18) and (27)] of dark solitons are exactly the same with conditions $k_1 = \sqrt{2\delta(a^2 + b^2)m_j^2}$. It is worth mentioning that, unlike the bright vector soliton, the soliton intensity affects on the time-dependent phase of dark vector soliton. The intensity and corresponding phase profiles for different values of blackness factor m_j are depicted in Fig. 3. It is evident that the phase of a dark soliton changes across the width, with a total phase shift of $2\sin^{-1}(m_j)$. For a black soliton ($m_j = 1$), a phase shift of π occurs exactly at the center of the dip. For the gray solitons ($m_j < 1$), phase varies gradually between $0 - \pi$.

IV. TWO-SOLITON SOLUTIONS

In order to get the bright vector two-soliton solution, the power-series expansions for G and F are truncated as follows: $G = g_1 + g_3$, $\bar{G} = h_1 + h_3$, and $F = 1 + f_2 + f_4$. Then, back to bilinear Eqs. (3), we obtain

$$g(z) = e^{-\int p(z)dz}$$

$$g_1 = \alpha_1 e^{\theta_1} + \alpha_2 e^{\theta_2}$$

$$g_3 = \sigma_1 e^{\theta_1 + \theta_1^* + \theta_2} + \sigma_2 e^{\theta_2 + \theta_2^* + \theta_1}$$

$$h_1 = \beta_1 e^{\theta_1} + \beta_2 e^{\theta_2}$$

$$h_3 = \varsigma_1 e^{\theta_1 + \theta_1^* + \theta_2} + \varsigma_2 e^{\theta_2 + \theta_2^* + \theta_1}$$

$$f_2 = \varrho_1 e^{\theta_1 + \theta_1^*} + \varrho_2 e^{\theta_1 + \theta_2^*} + \varrho_3 e^{\theta_2 + \theta_1^*} + \varrho_4 e^{\theta_2 + \theta_2^*}$$

$$f_4 = \varrho_5 e^{\theta_1 + \theta_1^* + \theta_2 + \theta_2^*}.$$

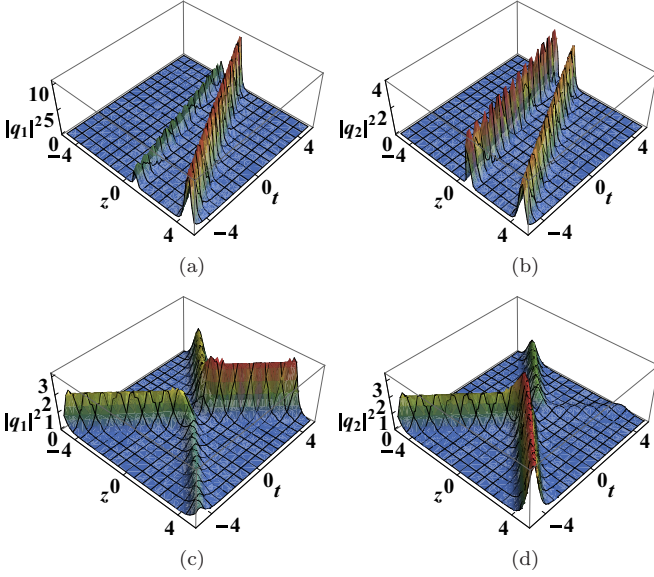


FIG. 6. The bright two-soliton propagation through homogenous fiber for parameters, (a) $\alpha_1 = 1 + 0.5i$, $\alpha_2 = 1 - 0.5i$; (b) $\beta_1 = 1$, $\beta_2 = 1 + 0.5i$ with $k_1 = 2 - i$, $k_2 = 2 - 2i$, $\phi_1 = -5$ and $\phi_2 = 5$. (c) Energy sharing collision with $\alpha_1 = 1$, $\alpha_2 = 1$; (d) $\beta_1 = 1$, $\beta_2 = 2 + i$ with $k_1 = 2 + 0.5i$, $k_2 = 2 - 0.5i$. Other physical quantities are $V(z) = 1$, $R(z) = 0.5$, and $p = 0$.

The final form of bright two-soliton solutions (for more details, see Appendix) can be written as

$$q_1(z, t) = e^{-\int p(z)dz} \frac{(g_1 + g_3)}{(1 + f_2 + f_4)}, \quad (28a)$$

$$q_2(z, t) = e^{-\int p(z)dz} \frac{(h_1 + h_3)}{(1 + f_2 + f_4)}. \quad (28b)$$

The above two-soliton solution is characterized by six arbitrary complex parameters α_1 , α_2 , β_1 , β_2 , k_1 , and k_2 . To construct the pair of dark two-soliton solutions, the power-series expansions for G , H , and F are truncated as follows: $G = g_0(1 + g_1 + g_2)$, $H = h_0(1 + h_1 + h_2)$, and $F = 1 + f_1 + f_2$. Then, from bilinear equations Eq. (3), we obtain

$$\begin{aligned} g_0 &= ae^{i\phi} & h_0 &= be^{i\phi} \\ g_1 &= \mu_1 e^{\theta_1} + \mu_2 e^{\theta_2} & h_1 &= \nu_1 e^{\theta_1} + \nu_2 e^{\theta_2} \\ g_2 &= A_{12} \mu_1 \mu_2 e^{\theta_1 + \theta_2} & h_2 &= A_{12} \nu_1 \nu_2 e^{\theta_1 + \theta_2} \\ f_1 &= e^{\theta_1} + e^{\theta_2} & f_2 &= A_{12} e^{\theta_1 + \theta_2}. \end{aligned}$$

(1) Before collision

$$(a) S^{1-}(\theta_1 + \theta_1^* \sim 0, \theta_2 + \theta_2^* \rightarrow -\infty)$$

$$\begin{pmatrix} q_1 \\ q_2 \end{pmatrix} \rightarrow \begin{pmatrix} S_1^{1-} \\ S_2^{1-} \end{pmatrix} = \begin{pmatrix} \alpha_1 \\ \beta_1 \end{pmatrix} \frac{e^{-\int p(z)dz}}{2\sqrt{\varrho_1}} e^{-i\theta_{1l}} \operatorname{sech}\left(\theta_{1R} + \frac{\ln \varrho_1}{2}\right), \quad (30)$$

$$(b) S^{2-}(\theta_2 + \theta_2^* \sim 0, \theta_1 + \theta_1^* \rightarrow \infty)$$

$$\begin{pmatrix} q_1 \\ q_2 \end{pmatrix} \rightarrow \begin{pmatrix} S_1^{2-} \\ S_2^{2-} \end{pmatrix} = \begin{pmatrix} \sigma_1 \\ \varsigma_1 \end{pmatrix} \frac{e^{-\int p(z)dz}}{2\sqrt{\varrho_1 \varrho_5}} e^{-i\theta_{2l}} \operatorname{sech}\left[\theta_{2R} + \frac{1}{2} \ln(\varrho_5 / \varrho_1)\right], \quad (31)$$

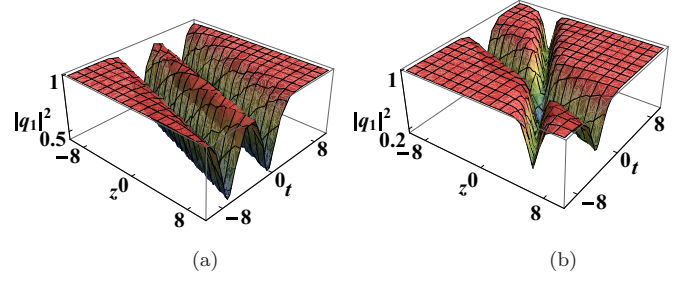


FIG. 7. The dark two-soliton propagation through homogenous fiber for parameters. (a) Same direction of propagation with $k_1 = k_2 = 1.5$, $\phi_1 = -5$, and $\phi_2 = 5$. (b) Soliton interaction with $k_1 = -1.5$, $k_2 = 1.5$, $\phi_1 = \phi_2 = 1$. Other physical quantities are $a = b = k = V(z) = \delta = 1$ and $p = 0$.

The final form of dark vector two-soliton solutions can be written as

$$q_1(z, t) = e^{-\int p(z)dz} \frac{g_0(1 + g_1 + g_2)}{(1 + f_1 + f_2)}, \quad (29a)$$

$$q_2(z, t) = e^{-\int p(z)dz} \frac{h_0(1 + h_1 + h_2)}{(1 + f_1 + f_2)}. \quad (29b)$$

By using Eqs. (28) and (29), we can investigate the propagation dynamics of vector solitons either in the same or opposite direction in a homogeneous or inhomogeneous fiber system. Figures 6 and 7 represent two-soliton solution in homogeneous systems. Comparing with the dark pulse, Manakov bright solitons have an additional feature, which exhibit the well-known energy exchange collision (for a detailed description, see Ref. [33]). The energy sharing collision of bright soliton are depicted in Figs. 6(c) and 6(d).

A. Asymptotic analysis and two-soliton phase

The behavior of head-on collision between the two-vector solitons in fibers can be analyzed by the asymptotic states of soliton solution. Based on the two-soliton solution, we can observe the elastic collision between bright and dark vector solitons. The asymptotic states of bright vector two-soliton solution Eq. (28) are introduced as follows:

(2) After collision

(a) $S^{1+}(\theta_1 + \theta_1^* \sim 0, \theta_2 + \theta_2^* \rightarrow \infty)$

$$\begin{pmatrix} q_1 \\ q_2 \end{pmatrix} \rightarrow \begin{pmatrix} S_1^{1+} \\ S_2^{1+} \end{pmatrix} = \begin{pmatrix} \sigma_2 \\ s_2 \end{pmatrix} \frac{e^{-\int p(z)dz}}{2\sqrt{\varrho_4\varrho_5}} e^{-i\theta_1 t} \operatorname{sech}\left[\theta_{1R} + \frac{1}{2} \ln(\varrho_5/\varrho_4)\right], \tag{32}$$

(b) $S^{2+}(\theta_2 + \theta_2^* \sim 0, \theta_1 + \theta_1^* \rightarrow -\infty)$

$$\begin{pmatrix} q_1 \\ q_2 \end{pmatrix} \rightarrow \begin{pmatrix} S_1^{2+} \\ S_2^{2+} \end{pmatrix} = \begin{pmatrix} \alpha_2 \\ \beta_2 \end{pmatrix} \frac{e^{-\int p(z)dz}}{2\sqrt{\varrho_4}} e^{-i\theta_2 t} \operatorname{sech}\left(\theta_{2R} + \frac{\ln \varrho_4}{2}\right). \tag{33}$$

Corresponding phase can be written as

$$\psi_j^{1-} = \frac{\delta(|\alpha_1|^2 + |\beta_1|^2)V(z)}{16\varrho_1} z, \tag{34}$$

$$\psi_j^{2-} = \frac{\delta(|\sigma_1|^2 + |s_1|^2)V(z)}{16\varrho_1\varrho_5} z, \tag{35}$$

$$\psi_j^{1+} = \frac{\delta(|\sigma_2|^2 + |s_2|^2)V(z)}{16\varrho_4\varrho_5} z, \tag{36}$$

$$\psi_j^{1-} = \frac{\delta(|\alpha_2|^2 + |\beta_2|^2)V(z)}{16\varrho_4} z. \tag{37}$$

The asymptotic analysis of dark vector two-soliton solutions given by Eq. (29) are conducted as follows:

(1) Before collision

(a) $S^{1-}(\theta_1 \sim 0, \theta_2 \rightarrow -\infty)$

$$\begin{pmatrix} q_1 \\ q_2 \end{pmatrix} \rightarrow \begin{pmatrix} S_1^{1-} \\ S_2^{1-} \end{pmatrix} = \begin{pmatrix} a \\ b \end{pmatrix} \frac{e^{i\psi}}{2e^{\int p(z)dz}} \left[(1 + \mu_1) + (\mu_1 - 1)\tanh\left(\frac{\theta_1}{2}\right) \right]. \tag{38}$$

(b) $S^{2-}(\theta_2 \sim 0, \theta_1 \rightarrow \infty)$

$$\begin{pmatrix} q_1 \\ q_2 \end{pmatrix} \rightarrow \begin{pmatrix} S_1^{2-} \\ S_2^{2-} \end{pmatrix} = \begin{pmatrix} a \\ b \end{pmatrix} \frac{\mu_1 e^{i\psi}}{2e^{\int p(z)dz}} \left[(1 + \mu_2) + (\mu_2 - 1)\tanh\left(\frac{\theta_2}{2} + \ln\sqrt{A_{12}}\right) \right]. \tag{39}$$

(2) After collision

(a) $S^{1+}(\theta_1 \sim 0, \theta_2 \rightarrow \infty)$

$$\begin{pmatrix} q_1 \\ q_2 \end{pmatrix} \rightarrow \begin{pmatrix} S_1^{1+} \\ S_2^{1+} \end{pmatrix} = \begin{pmatrix} a \\ b \end{pmatrix} \frac{\mu_2 e^{i\psi}}{2e^{\int p(z)dz}} \left[(1 + \mu_1) + (\mu_1 - 1)\tanh\left(\frac{\theta_1}{2} + \ln\sqrt{A_{12}}\right) \right]. \tag{40}$$

(b) $S^{2+}(\theta_2 \sim 0, \theta_1 \rightarrow -\infty)$

$$\begin{pmatrix} q_1 \\ q_2 \end{pmatrix} \rightarrow \begin{pmatrix} S_1^{2+} \\ S_2^{2+} \end{pmatrix} = \begin{pmatrix} a \\ b \end{pmatrix} \frac{e^{i\psi}}{2e^{\int p(z)dz}} \left[(1 + \mu_2) + (\mu_2 - 1)\tanh\left(\frac{\theta_2}{2}\right) \right] \tag{41}$$

with the condition $k_j = \sqrt{2\delta(a^2 + b^2)m_j^2}$, corresponding phase can be written as

$$\psi_j^{1-} = \sqrt{\frac{\delta}{2}(a^2 + b^2)(1 - (m_j^{1-})^2)} t + \tan^{-1} \left\{ \frac{m_j^{1-} \tanh\left[\sqrt{\frac{\delta}{2}(a^2 + b^2)m_j^{1-} t + \frac{\phi_1}{2}}\right]}{\sqrt{1 - (m_j^{1-})^2}} \right\} + \frac{\sqrt{1 - (m_j^{1-})^2}}{2m_j^{1-}} \phi_1 + \Omega_j^{1-} z, \tag{42}$$

$$\begin{aligned} \psi_j^{2-} = & \sqrt{\frac{\delta}{2}(a^2 + b^2)[1 - (m_j^{2-})^2]}t + \tan^{-1} \left\{ \frac{m_j^{2-} \tanh[\sqrt{\frac{\delta}{2}(a^2 + b^2)m_j^{2-}t + \frac{\phi_2}{2} + \ln\sqrt{A_{12}}]} }{\sqrt{1 - (m_j^{2-})^2}} \right\} \\ & + \frac{\sqrt{1 - (m_j^{2-})^2}}{2m_j^{2-}}(\phi_2 + \ln[A_{12}]) + \Omega_j^{2-}z, \end{aligned} \quad (43)$$

$$\begin{aligned} \psi_j^{1+} = & \sqrt{\frac{\delta}{2}(a^2 + b^2)[1 - (m_j^{1+})^2]}t + \tan^{-1} \left\{ \frac{m_j^{1+} \tanh[\sqrt{\frac{\delta}{2}(a^2 + b^2)m_j^{1+}t + \frac{\phi_1}{2} + \ln\sqrt{A_{12}}]} }{\sqrt{1 - (m_j^{1+})^2}} \right\} \\ & + \frac{\sqrt{1 - (m_j^{1+})^2}}{2m_j^{1+}}(\phi_1 + \ln[A_{12}]) + \Omega_j^{1+}z, \end{aligned} \quad (44)$$

$$\psi_j^{2+} = \sqrt{\frac{\delta}{2}(a^2 + b^2)[1 - (m_j^{2+})^2]}t + \tan^{-1} \left\{ \frac{m_j^{2+} \tanh[\sqrt{\frac{\delta}{2}(a^2 + b^2)m_j^{2+}t + \frac{\phi_2}{2}]} }{\sqrt{1 - (m_j^{2+})^2}} \right\} + \frac{\sqrt{1 - (m_j^{2+})^2}}{2m_j^{2+}}\phi_2 + \Omega_j^{2+}z, \quad (45)$$

where

$$\begin{aligned} (m_1^{j-})^2 &= \frac{(B_1^{j-})^2}{a^2} e^{2 \int p(z) dz}, & (m_2^{j-})^2 &= \frac{(B_2^{j-})^2}{b^2} e^{2 \int p(z) dz} \\ (m_1^{j+})^2 &= \frac{(B_1^{j+})^2}{a^2} e^{2 \int p(z) dz}, & (m_2^{j+})^2 &= \frac{(B_2^{j+})^2}{b^2} e^{2 \int p(z) dz} \\ \left(\begin{matrix} B_1^{1-} \\ B_2^{1-} \end{matrix} \right) &= \begin{pmatrix} a \\ b \end{pmatrix} \left| \frac{(\mu_1 - 1)}{2e^{\int p(z) dz}} \right|, & \left(\begin{matrix} B_1^{2-} \\ B_2^{2-} \end{matrix} \right) &= \begin{pmatrix} a \\ b \end{pmatrix} \left| \frac{\mu_1(\mu_2 - 1)}{2e^{\int p(z) dz}} \right| \\ \left(\begin{matrix} B_1^{1+} \\ B_2^{1+} \end{matrix} \right) &= \begin{pmatrix} a \\ b \end{pmatrix} \left| \frac{\mu_2(\mu_1 - 1)}{2e^{\int p(z) dz}} \right|, & \left(\begin{matrix} B_1^{2+} \\ B_2^{2+} \end{matrix} \right) &= \begin{pmatrix} a \\ b \end{pmatrix} \left| \frac{(\mu_2 - 1)}{2e^{\int p(z) dz}} \right|. \end{aligned}$$

From the above asymptotic expressions for collision, we can identify that total energy is conserved during the interaction process. The resultant intensity of bright vector soliton due to energy sharing collisions and the corresponding phases are depicted in Fig. 8. It is obvious that the resultant phase of bright solitons remains unchanged during the collision. But in the case of the dark soliton, the phase behaves markedly different from the bright soliton case. Here we have studied the phase profile of two gray vector solitons as shown in Fig. 9. When both soliton travel in the same direction, the resultant phase produce a net phase shift equal to the sum of individual phase shift as shown in Fig. 9(b). Figure 9(d) represents the phase profile of two oppositely moving gray soliton before the collision and the recovered phase after the collision is depicted in Fig. 9(h). It is evident that the solitons recover the phase after the collision and maintains its phase shift [35]. At the point of collision the phase profiles of the two solitons cancel each other as shown in the Fig. 9(f).

V. RESULTS AND DISCUSSIONS

In previous sections, the Manakov model and its pair of vector soliton with a constant mode of propagation have been discussed in detail. Especially, the corresponding phase profile of vector solitons has been emphasized explicitly for the first time to the best of our knowledge. Recently, the intensity of

Manakov vector soliton with varying coefficients is studied in Refs. [34,39]. But the actual phase profile of bright and dark vector solitons in the CNLSE or Vc-CNLSE models are not addressed yet. Here we report the inhomogeneous effects on soliton intensity and the corresponding phase of the Manakov bright and dark vector solitons.

When considering a periodically varying GVD parameter [48,49], solitons exhibit oscillating phase variation along the spatial axis, while the amplitude and width of vector solitons remain constant. The effect of GVD parameter [$V(z) = \cos(0.7z)$] in one and two bright solitons dynamics are depicted in Fig. 10. In contrast to the concept of constant phase

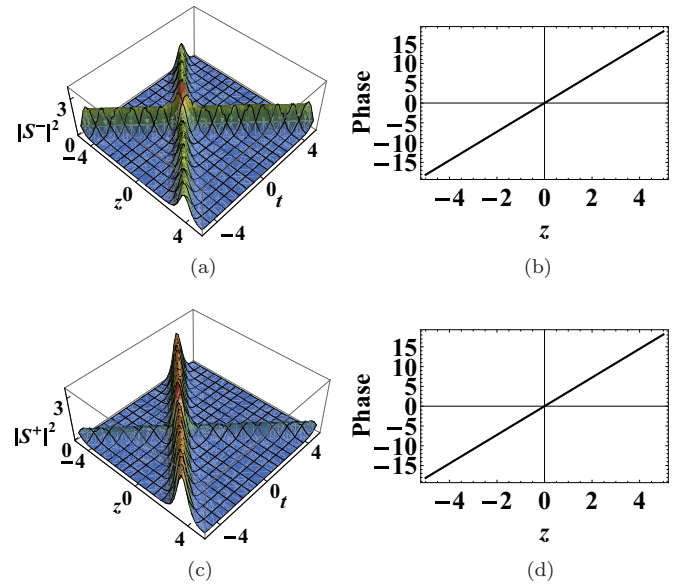


FIG. 8. The bright two-soliton energy sharing collision via the asymptotic expression. (a) Before collision $S^- = S_1^- + S_2^-$. (b) Corresponding phase with $\psi_1^- + \psi_2^-$ (c) after collision $S^+ = S_1^+ + S_2^+$. (d) Corresponding phase with $\psi_1^+ + \psi_2^+$. Other physical quantities are $\alpha_1 = 1$, $\alpha_2 = 1$, $k_1 = 2 + 0.5i$, $k_2 = 2 - 0.5i$, $V(z) = 1$, $R(z) = 0.5$, and $p = 0$.

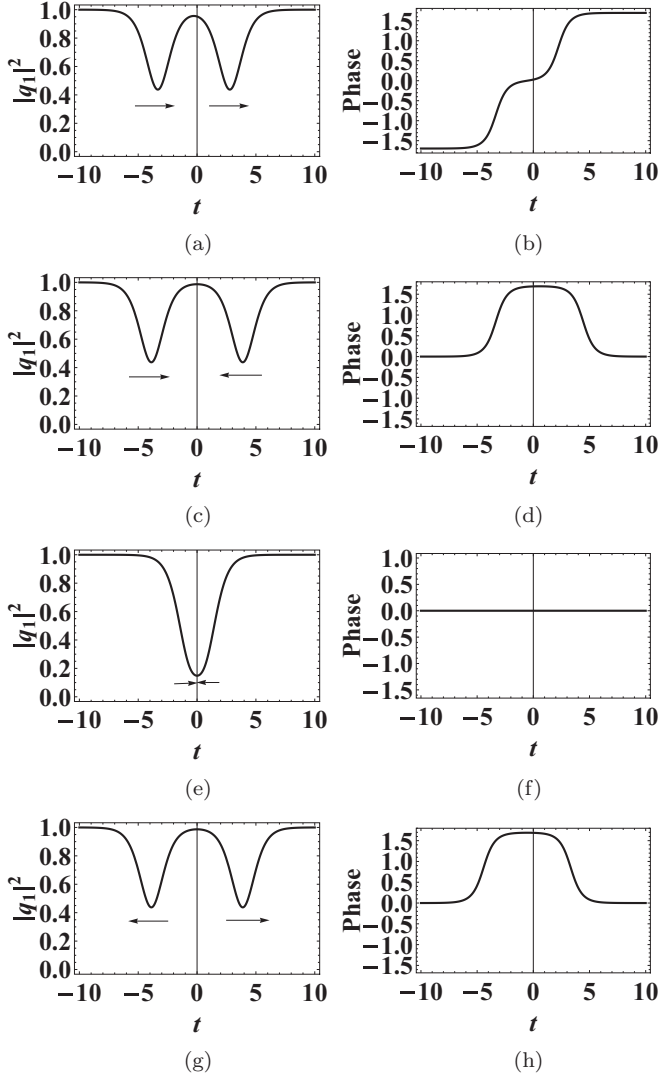


FIG. 9. The resultant intensity and phase of two dark soliton via the asymptotic expressions for before and after collision (a) same direction of propagation with $k_1 = 1.5$ and $k_2 = 1.5$, $\phi_1 = 5$, and $\phi_2 = -5$. (b) Corresponding phase (c) before collision with $k_1 = -1.5$ and $k_2 = 1.5$, $\phi_1 = 5$, and $\phi_2 = 5$. (d) Corresponding phase (e) at collision with $k_1 = -1.5$ and $k_2 = 1.5$, $\phi_1 = \phi_2 = 0$. (f) Corresponding phase. (g) After collision with $k_1 = 1.5$ and $k_2 = -1.5$, $\phi_1 = 5$, and $\phi_2 = 5$. (h) Corresponding phase. Other relevant physical parameters are $k_0 = a = V(z) = 1$, $p = 0$, and $R = 0.5$.

of bright soliton in the NLSE [1], the $V(z)$ plays a significant role in the evolutionary dynamics of soliton phase in varying coefficients models.

In the presence of medium gain or loss, soliton intensity undergoes amplification or absorption. When $p(z)$ is a constant value as $p = -0.02$ ($p = 0.02$), medium exhibits constant gain (loss). The effect of gain (loss) on dark solitons phase is depicted in Fig. 11. It is quite evident that the dark soliton phase gradually decreases (increases) with respect to the medium gain (loss). This is attributed to the fact that the soliton intensity varies inversely with the actual phase of the dark soliton. During the time of amplification (absorption), soliton intensity increases (decreases) correspondingly, which

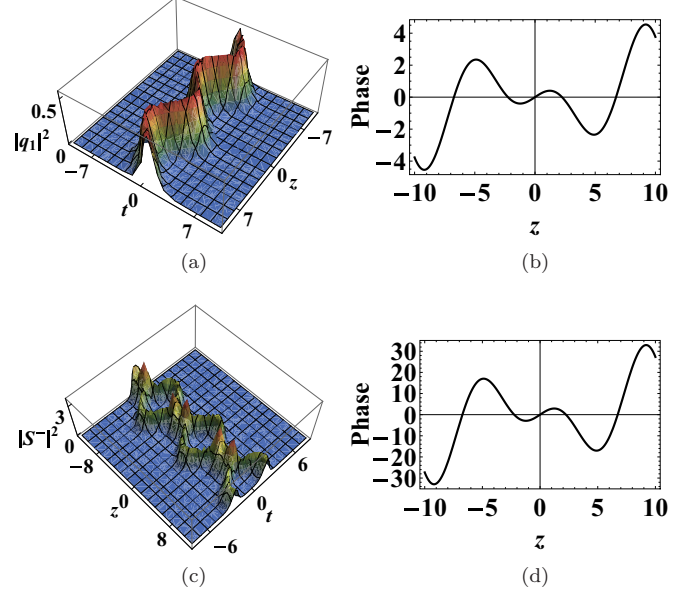


FIG. 10. The bright soliton propagation with varying GVD parameter, where $V(z) = R(z) = \cos(0.7z)$. (a) One soliton with $k_1 = 1 + i$, $\alpha_1 = 1 + i$, $\beta_1 = 2 - i$, $R(z) = 0.5$, and $p = 0$. (b) Corresponding phase. (c) Two-soliton with $\alpha_1 = 1$, $\alpha_2 = 1$, $k_1 = 2 + 0.5i$, $k_2 = 2 - 0.5i$, and $p = 0$. (d) Corresponding phase.

reduces (raises) the total phase shift of dark soliton spatially as shown in Figs. 11(b) and 11(d). The phase evolution due to influence of background oscillation [$p = 0.05 \sin(z)$] is depicted in Fig. 11(f). In similar lines with the dark one-soliton situations, we extended the phase dynamics of the two-soliton solutions as shown in Fig. 12. Unlike the bright two-soliton which has the same resultant phase before and after collision, a dark soliton exhibits different forms of resultant phase shift due to the mode of two-soliton propagation. The medium inhomogeneity and corresponding phase change in the same direction of propagation is depicted in Figs. 12(a), 12(c), and 12(e). The phase variation of a dark soliton due to the interactions between the two solitons are depicted (with same inhomogeneity) in Figs. 12(b), 12(d), and 12(f).

A. Nonlinear tunneling and soliton phase

In the recent past, the nonlinear tunneling phenomenon of solitons have been explored in many leading research works [34,50–53]. The first experimental achievement of tunneling phenomena through a potential barrier was reported in Ref. [54]. To investigate nonlinear tunneling effect of the Manakov vector soliton through the dispersion barrier or well, we choose the parameter as follows [44,50]:

$$V(z) = r_0 \pm h \operatorname{sech}^2[c(z - z_0)]$$

$$R(z) = R_0,$$

where $\pm h$ indicates the height of the barrier or well. The parameter c is related to its width and z_0 indicates the location of the dispersion barrier or well and R_0 is a constant parameter. When a bright (dark) soliton propagates through the dispersion barrier, the intensity (blackness) of the pulse grows and forms a peak at the barrier location and retains its

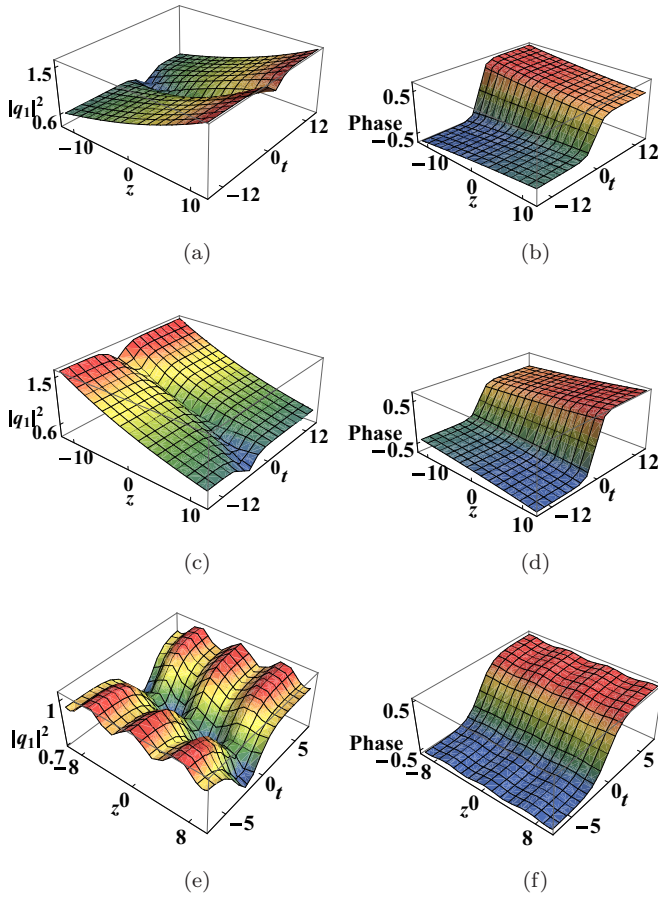


FIG. 11. The dark vector soliton propagation through inhomogeneous fiber for parameters. (a) Pulse amplification (gain) with $p = -0.02$. (b) Corresponding phase. (c) Pulse absorption (loss) with $p = 0.02$. (d) Corresponding phase. (e) Periodic background as $p = 0.05\sin(z)$. (f) Corresponding phase. Other physical quantities are $k = V(z) = 1, R = 0.5$.

shape after crossing the barrier. Similarly, when a bright (dark) soliton propagates through the dispersion well the intensity (blackness) of the pulse diminishes and a valley is formed at $z = z_0$ and restores its shape after crossing through the well. In this work, apart from the intensity or blackness of tunneling soliton, we exclusively studied the corresponding phase change of vector soliton when it passes through the dispersion barrier and well.

The Manakov bright soliton propagation through dispersion barrier and the corresponding phase change are illustrated in Figs. 13(a) and 13(b), respectively. Similarly, the soliton passing through dispersion well and corresponding phase change are respectively depicted in Figs. 13(c) and 13(d). It is evident that at the region of the barrier, the phase becomes steeper and maintains its original phase. But in the case of dispersion well, the phase vanishes at well and retains its actual phase after crossing the given well.

The dark soliton propagation through dispersion barrier and corresponding phase change are portrayed in Figs. 14(a) and 14(b), respectively. When dark soliton pass through the dispersion barrier, the maximum phase shift takes place at the region of the barrier and then it retains its original form.

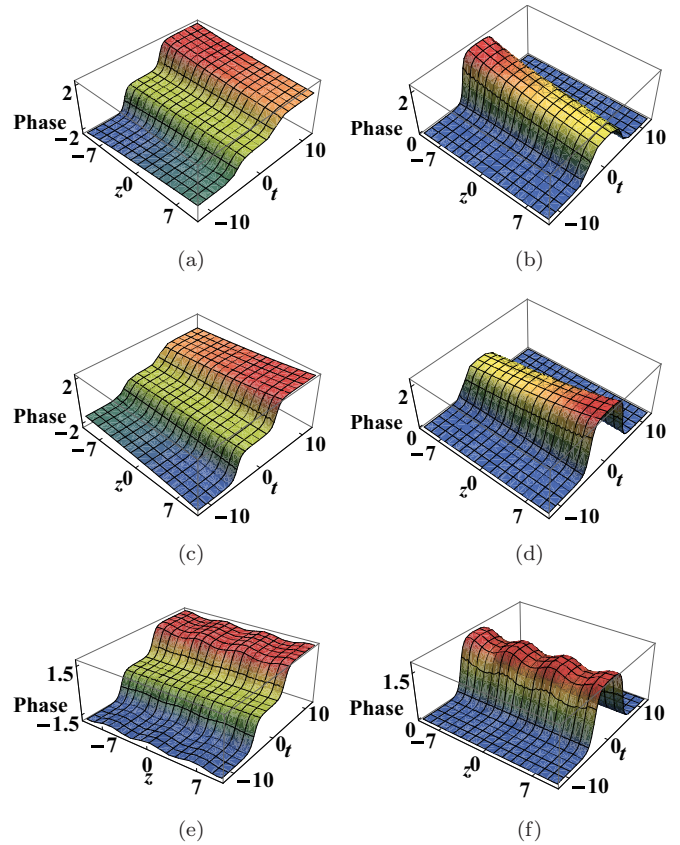


FIG. 12. The dark two-soliton phase via the asymptotic expressions (a) gain of two-soliton with same direction of propagation. (b) Gain of two-soliton with opposite direction of propagation. (c) Loss of two-soliton with same direction of propagation. (d) Loss of two-soliton with opposite direction of propagation. (e) Periodic background in two-solitons for the same direction of propagation. (f) Periodic background in two-solitons for the opposite direction of propagation. Where same direction of propagation studied with parameter $k_1 = 1.5, k_2 = 1.5, \phi_1 = -5$, and $\phi_2 = 5$, for the interactive mode $k_1 = -1.5, k_2 = 1.5, \phi_1 = 5$, and $\phi_2 = 5$. Other relevant physical quantities are $k_0 = a = 1$ and $R = 0.5$.

Similarly, dark soliton propagation through dispersion well and corresponding phase change are respectively depicted in Figs. 14(c) and 14(d). In the case of a well, the phase vanishes at the region of the well and retains its original shape after passing through it. For better insight, the nonlinear tunneling effect on the Manakov dark two-solitons is shown in Fig. 15, where the same direction and interactive mode of propagation of two-soliton are considered.

VI. SUMMARY AND CONCLUSION

In summary, we have investigated the phase dynamics of the Manakov bright and dark vector solitons in inhomogeneous fibers by employing a two-component Vc-CNLS model. The exact one- and two-soliton solutions have been derived by Hirota’s bilinear method. To study the phase dynamics of the system, we have applied a general ansatz method which enabled explicit analytical expressions for intensity as well as the phase of the soliton. By equating the

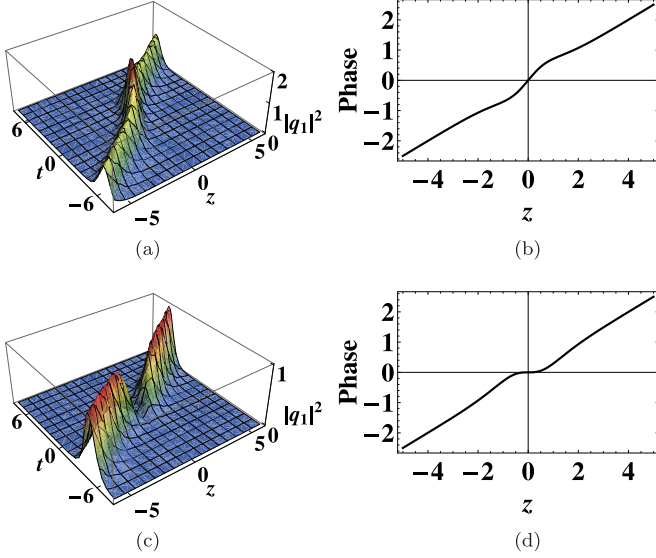


FIG. 13. The bright vector soliton tunneling for parameters. (a) Dispersion barrier with $V(z) = 1 + h \operatorname{sech}[z - z_0]^2$ and $h = 1$. (b) Corresponding phase. (c) Dispersion well with $h = -1$. (d) Corresponding phase. Other relevant physical quantities are $k_1 = 1 + i$, $\alpha_1 = 1 + i$, $\beta_1 = 1 - i$, $R(z) = 0.5$, $z_0 = 0$, and $p = 0$.

unknown parameters of this ansatz with the exact solutions of the well-known HB method, we have obtained the exact phase of the Manakov soliton. Numerical simulations were performed and both the bright and dark soliton solutions show remarkable stability against perturbation. By using the asymptotic analysis of two-soliton solutions, the phase of the individual solitons has been explored. Unlike the bright vector soliton which has a constant phase in a homogeneous

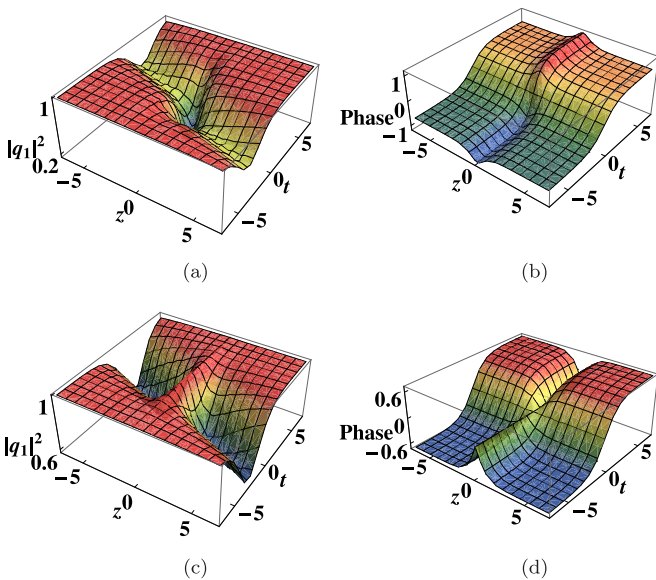


FIG. 14. The dark vector soliton tunneling for parameters. (a) Dispersion barrier with $V(z) = 1 + h \operatorname{sech}[z - z_0]^2$ and $h = 1$. (b) Corresponding phase. (c) Dispersion well with $h = -1$. (d) Corresponding phase. Other physical quantities are $k_0 = k_1 = a = 1$, $R(z) = 0.3$, and $z_0 = 0$.

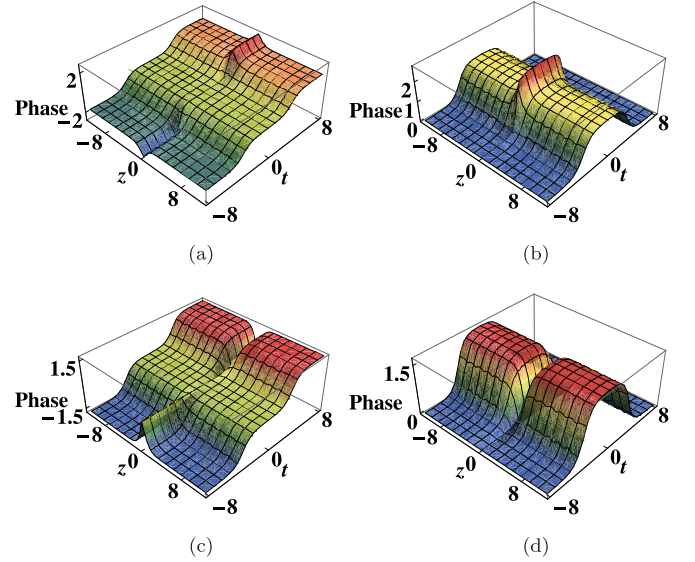


FIG. 15. The phase change of dark two-soliton and tunneling effect for parameter $V(z) = 1 + h \operatorname{sech}[z - z_0]^2$. (a) Dispersion barrier in same direction mode with $h = 0.7$. (b) Dispersion barrier in opposite direction mode with $h = 0.7$. (c) Dispersion well in same direction mode with $h = -1$. (d) Dispersion well in opposite direction mode with $h = -1$, where the same direction of propagation studied with parameter $k_1 = 1.5$, $k_2 = 1.5$, $\phi_1 = -5$, and $\phi_2 = 5$ for the opposite mode $k_1 = -1.5$, $k_2 = 1.5$, $\phi_1 = \phi_2 = 5$. Other physical quantities are $k_0 = a = 1$, $R(z) = 0.5$, and $z_0 = 0$.

medium, the time-dependent phase of a dark soliton exhibits a gradual phase change. The influence of varying coefficients such as periodically varying GVD, medium gain or loss, and background oscillations on the dynamics of phase evolution have also been discussed in detail, to the two-soliton level. Moreover, we have studied the nonlinear tunneling effect of Manakov soliton in the context of dispersion barrier or well. When soliton pass through the dispersion barrier (well), the maximum (minimum) phase change takes place at the region of barrier (well) and the phase retains its original form after crossing the given barrier (well).

To conclude, in contrast to the conventional intensity-based soliton description, we have presented a comprehensive analysis of the phase dynamics of the soliton in a self-explanatory way. Unlike the common usage of the Hirota's bilinear method for soliton intensity, we have extended the capability of the HB method in understanding the phase profile of the multisoliton solutions. As is known, the phase profile has a significant role in multisoliton solutions, especially in the bound-state soliton system, where the relative phase plays a significant role in explaining the nature of the vector soliton interaction, such as attractive or repulsive. We believe the aforementioned results in this paper can serve as a potential reference for many future studies related to the phase dynamics of more complex systems.

ACKNOWLEDGMENTS

N.M.M. thanks UGC-MANF, Government of India, for the financial support through SRF. P.A.S. thanks DST-FIST, Government of India, for the financial support.

APPENDIX: COEFFICIENTS OF TWO-SOLITON

Here we give more details of obtained coefficients of two-soliton solution. For the bright two soliton,

$$\theta_1 = k_1 t - \omega_1 \int V(z) dz + \phi_1$$

$$\theta_2 = k_2 t - \omega_2 \int V(z) dz + \phi_2$$

$$\varrho_1 = \frac{\delta(\alpha_1 \alpha_1^* + \beta_1 \beta_1^*)}{2(k_1 + k_1^*)^2}$$

$$\varrho_2 = \frac{\delta(\alpha_1 \alpha_2^* + \beta_1 \beta_2^*)}{2(k_1 + k_2^*)^2}$$

$$\varrho_3 = \frac{\delta(\alpha_1^* \alpha_2 + \beta_1^* \beta_2)}{2(k_1^* + k_2)^2}$$

$$\varrho_4 = \frac{\delta(\alpha_2 \alpha_2^* + \beta_2 \beta_2^*)}{2(k_2 + k_2^*)^2}$$

$$\sigma_1 = (k_1 - k_2) \left(\frac{\alpha_1 \rho_3}{k_1 + k_1^*} - \frac{\alpha_2 \rho_1}{k_2 + k_1^*} \right)$$

$$\sigma_2 = (k_1 - k_2) \left(\frac{\alpha_1 \rho_4}{k_1 + k_2^*} - \frac{\alpha_2 \rho_2}{k_2 + k_2^*} \right)$$

$$\varsigma_1 = (k_1 - k_2) \left(\frac{\beta_1 \rho_3}{k_1 + k_1^*} - \frac{\beta_2 \rho_1}{k_2 + k_1^*} \right)$$

$$\varsigma_2 = (k_1 - k_2) \left(\frac{\beta_1 \rho_4}{k_1 + k_2^*} - \frac{\beta_2 \rho_2}{k_2 + k_2^*} \right)$$

$$\varrho_5 = \frac{\delta(|\alpha_1|^2 |\alpha_2|^2 + |\beta_1|^2 |\beta_2|^2) |k_1 - k_2|^4}{4(k_1 + k_1^*)(k_2 + k_2^*) |k_1 + k_2|^4}$$

for the two dark solitons solution,

$$g_0 = a e^{i\phi},$$

$$h_0 = b e^{i\phi}$$

$$\phi = k_0 t - \omega_0 \int V(z) dz,$$

$$g(z) = e^{-\int p(z) dz}$$

$$\lambda = \frac{1}{2} \delta(a^2 + b^2) V(z),$$

$$\omega_0 = -\frac{\lambda}{V(z)} - \frac{k_0^2}{2}$$

$$\alpha_1 = \frac{2\omega_1 + 2kk_1 + ik_1^2}{2\omega_1 + 2kk_1 - ik_1^2},$$

$$\beta_1 = \alpha_1$$

$$\alpha_2 = \frac{2\omega_2 + 2kk_2 + ik_2^2}{2\omega_2 + 2kk_2 - ik_2^2},$$

$$\beta_2 = \alpha_2$$

$$\theta_1 = k_1 t - \omega_1 \int V(z) dz + \phi_1$$

$$\theta_2 = k_2 t - \omega_2 \int V(z) dz + \phi_2$$

$$\omega_1 = \frac{k_1}{2} \left[-2k \pm \sqrt{2\delta(a^2 + b^2) - k_1^2} \right]$$

$$\omega_2 = \frac{k_2}{2} \left[-2k \pm \sqrt{2\delta(a^2 + b^2) - k_2^2} \right]$$

$$A_{12} = -\frac{2i(\alpha_1 - \alpha_2)(\omega_2 - \omega_1 - kk_1 + kk_2) - (\alpha_1 + \alpha_2)(k_1 - k_2)^2}{2i(1 - \alpha_1 \alpha_2)(\omega_1 + \omega_2 + kk_1 + kk_2) - (\alpha_1 \alpha_2 + 1)(k_1 + k_2)^2}.$$

- [1] G. P. Agrawal, *Nonlinear Fiber Optics* (Academic Press, New York, 2013).
- [2] C. R. Menyuk, *Opt. Lett.* **12**, 614 (1987).
- [3] A. Hasegawa and Y. Kodama, *Solitons in Optical Communications* (Oxford University Press, Oxford, 1995).
- [4] Y. S. Kivshar and G. P. Agrawal, *Optical Solitons from Fibers to Photonic Crystals* (Academic Press, New York, 2003).
- [5] A. Hasegawa and F. D. Tappert, *Appl. Phys. Lett.* **23**, 142 (1973).
- [6] L. F. Mollenauer, R. H. Stolen, and J. P. Gordon, *Phys. Rev. Lett.* **45**, 1095 (1980).
- [7] Y. S. Kivshar and B. Luther-Davies, *Phys. Rep.* **298**, 81 (1998).
- [8] P. Emplit, J. P. Hamaide, F. Reynaud, and A. Barthelemy, *Opt. Commun.* **62**, 374 (1987).
- [9] A. M. Weiner, J. P. Heritage, R. J. Hawkins, R. N. Thurston, E. M. Kirschner, D. E. Leaird, and W. J. Tomlinson, *Phys. Rev. Lett.* **61**, 2445 (1988).
- [10] Yuri S. Kivshar *et al.*, *Chaos, Solitons Fract.* **4**, 1745 (1994).
- [11] M. N. Islam, C. D. Poole, and J. P. Gordon, *Opt. Lett.* **14**, 1011 (1989).
- [12] D. N. Christodoulides, S. R. Singh, M. I. Carvalho, and M. Segev, *Appl. Phys. Lett.* **68**, 1763 (1996).
- [13] Z. Chen, M. Segev, T. Coskun, and D. N. Christodoulides, *Opt. Lett.* **21**, 1436 (1996).
- [14] C. R. Menyuk, *IEEE J. Quant. Electron.* **25**, 2674 (1989).
- [15] D. J. Kaup and B. A. Malomed, *Phys. Rev. A* **48**, 599 (1993).
- [16] S. V. Manakov, *Zh. Eksp. Teor. Fiz.* **65**, 505 (1973) [*Sov. Phys. JETP* **38**, 248 (1974)].
- [17] C. Anastassiou, M. Segev, K. Steiglitz, J. A. Giordmaine, M. Mitchell, M. F. Shih, S. Lan, and J. Martin, *Phys. Rev. Lett.* **83**, 2332 (1999).
- [18] C. Anastassiou, J. W. Fleischer, T. Carmon, M. Segev, and K. Steiglitz, *Opt. Lett.* **26**, 1498 (2001).
- [19] M. Shih and M. Segev, *Opt. Lett.* **21**, 1538 (1996).
- [20] J. U. Kang, G. I. Stegeman, J. S. Aitchison, and N. Akhmediev, *Phys. Rev. Lett.* **76**, 3699 (1996).
- [21] V. V. Steblina, A. V. Buryak, R. A. Sammut, D. Y. Zhou, M. Segev, and P. Prucnal, *J. Opt. Soc. Am. B* **17**, 2026 (2000).
- [22] E. P. Bashkin and A. V. Vagov, *Phys. Rev. B* **56**, 6207 (1997).

- [23] B. Frisquet, B. Kibler, J. Fatome, P. Morin, F. Baronio, M. Conforti, G. Millot, and S. Wabnitz, *Phys. Rev. A* **92**, 053854 (2015).
- [24] R. Radhakrishnan, M. Lakshmanan, and J. Hietarinta, *Phys. Rev. E* **56**, 2213 (1997).
- [25] M. N. Islam, *Ultrafast Fiber Switching Devices and Systems* (Cambridge University Press, New York, 1992).
- [26] M. H. Jakubowski, K. Steiglitz, and R. Squier, *Phys. Rev. E* **58**, 6752 (1998).
- [27] K. Steiglitz, *Phys. Rev. E* **63**, 016608 (2000).
- [28] D. Rand, K. Steiglitz, and P. R. Prucnal, *Int. J. Unconv. Comp.* **1**, 31 (2005).
- [29] D. Rand, K. Steiglitz, and P. R. Prucnal, *Phys. Rev. A* **71**, 053805 (2005).
- [30] J. Yang, *Phys. Rev. E* **59**, 2393 (1999).
- [31] R. Radhakrishnan and M. Lakshmanan, *J. Phys. A: Math. Gen.* **28**, 2683 (1995).
- [32] T. Kanna and M. Lakshmanan, *Phys. Rev. Lett.* **86**, 5043 (2001).
- [33] T. Kanna and M. Lakshmanan, *Phys. Rev. E* **67**, 046617 (2003).
- [34] N. M. Musammil, K. Porsezian, P. A. Subha, and K. Nithyanandan, *Chaos* **27**, 023113 (2017).
- [35] I. Gabitov, E. G. Shapiro, and S. K. Turitsyn, *Phys. Rev. E* **55**, 3624 (1997).
- [36] V. N. Serkin and A. Hasegawa, *Phys. Rev. Lett.* **85**, 4502 (2000).
- [37] V. I. Kruglov, A. C. Peacock, and J. D. Harvey, *Phys. Rev. Lett.* **90**, 113902 (2003).
- [38] C. G. Latchio Tiofacka, A. Mohamadoub, T. C. Kofané, and K. Porsezian, *J. Mod. Opt.* **57**, 261 (2010).
- [39] S. Chakraborty, S. Nandy, and A. Barthakur, *Phys. Rev. E* **91**, 023210 (2015).
- [40] Y. Yang, Z. Yan, and D. Mihalache, *J. Math. Phys.* **56**, 053508 (2015).
- [41] R. Hirota, *The Direct Method in Soliton Theory* (Cambridge University Press, Cambridge, 2004).
- [42] K. Porsezian and K. Nakkeeran, *Phys. Rev. Lett.* **76**, 3955 (1996).
- [43] W. J. Liu, B. Tian, H. Q. Zhang, T. Xu, and H. Li, *Phys. Rev. A* **79**, 063810 (2009).
- [44] N. M. Musammil, K. Porsezian, K. Nithyanandan, P. A. Subha, and P. Tchofo Dinda, *Opt. Fiber Technol.* **37**, 11 (2017).
- [45] R. N. Thurston and A. M. Weiner, *J. Opt. Soc. Am. B* **8**, 471 (1991).
- [46] D. Foursa and P. Emplit, *Phys. Rev. Lett.* **77**, 4011 (1996).
- [47] N. M. Musammil, P. A. Subhab, and K. Nithyanandan, *Optik* **159**, 176 (2018).
- [48] B. A. Malomed, *Soliton Management in Periodic Systems* (Springer, Berlin, 2006).
- [49] K. Porsezian, A. Hasegawa, V. N. Serkin, T. L. Belyaeva, and R. Ganapathy, *Phys. Lett. A* **361**, 504 (2007).
- [50] A. C. Newell, *J. Math. Phys.* **19**, 1126 (1978).
- [51] V. N. Serkin and T. L. Belyaeva, *J. Exp. Theor. Phys. Lett.* **74**, 573 (2001).
- [52] C. Q. Dai, Y. Y. Wang, and J. F. Zhang, *Opt. Express* **18**, 17548 (2010).
- [53] T. L. Belyaeva and V. N. Serkin, *Eur. Phys. J. D* **66**, 153 (2012).
- [54] A. Barak, O. Peleg, C. Stucchio, A. Soffer, and M. Segev, *Phys. Rev. Lett.* **100**, 153901 (2008).